PROCEEDINGS OF SPIE

SPIEDigitalLibrary.org/conference-proceedings-of-spie

Label-free photoacoustic microscopy of cytochrome c in cells

Chi Zhang, Yu Zhang, Da-Kang Yao, Younan Xia, Lihong V. Wang

Chi Zhang, Yu Zhang, Da-Kang Yao, Younan Xia, Lihong V. Wang, "Label-free photoacoustic microscopy of cytochrome c in cells," Proc. SPIE 8223, Photons Plus Ultrasound: Imaging and Sensing 2012, 82231W (23 February 2012); doi: 10.1117/12.906202

SPIE.

Event: SPIE BiOS, 2012, San Francisco, California, United States

Label-free photoacoustic microscopy of cytochrome *c* in cells

Chi Zhang, Yu Zhang, Da-Kang Yao, Younan Xia, and Lihong V. Wang*
Department of Biomedical Engineering, Washington *University in St. Louis, One Brookings Drive, St. Louis, MO 63130, USA*
* Corresponding author: lhwang@biomed.wustl.edu

ABSTRACT

Cytochrome *c* is a heme protein normally bound to mitochondria and is important for mitochondrial electron transport and apoptosis initiation. Since cytochrome *c* is nonfluorescent, it is always labeled with fluorescent molecules for imaging, which, however, may affect normal cellular functions. Here, label-free photoacoustic microscopy (PAM) of mitochondrial cytochrome *c* was realized for the first time by utilizing the optical absorption around the Soret peak. PAM was demonstrated to be sensitive enough to image mitochondrial cytochrome *c* at 422 nm wavelength. Mitochondrial cytochrome *c* in the cytoplasm of fixed fibroblasts was clearly imaged by PAM as confirmed by fluorescent labeling. By showing mitochondrial cytochrome *c* in various cells, we demonstrated the feasibility of PAM for label-free histology of mouse ear sections. Therefore, PAM can sensitively image cytochrome c in unstained cells at 422 nm wavelength and has great potential for functional imaging of cytochrome *c* in live cells or *in vivo*.

Keywords: photoacoustic microscopy, cytochrome *c*, label-free

1. INTRODUCTION

Cytochrome *c* is a heme protein normally bound to mitochondria and is a necessary component for lots of cellular functions. For example, cytochrome *c* is required for mitochondrial electron transport[1], during which it may exist in the oxidized form or reduced form. Cytochrome *c* is also required for apoptosis initiation[2]. Recently, hot research topic focuses on the functional role cytochrome *c* takes in apoptosis regulation when it is released from mitochondria[3],[4]. Nearly all these studies need to image cytochrome *c* and mitochondria dynamically in live cells.

Among all the imaging technologies, optical imaging technologies have been most commonly used for real-time monitoring of live cells, including cytochrome *c* studies. Cytochrome *c* is nonfluorescent and weakly-scattering, so fluorescent probes (e.g., Mitotracker® probes) are always used to label the cytochrome *c* in cells for imaging. However, the normal functions of biomolecules are sometimes disturbed by the labeling. For example, it has been shown that mitochondrial permeability and respiration can be affected by Mitotracker® labeling[5],[6]. Without labeling, cytochrome *c* in live cells have been imaged by photothermal technologies[7],[8] and analyzed by spectrophotometric technologies[9],[10]. These studies show that cytochrome *c* is a major endogenous source of optical absorption in cells at its absorption peaks (e.g., around 415 nm, 520 nm, and 550 nm for reduced cytochrome *c*).

Photoacoustic microscopy (PAM) can be suitable for label-free imaging of mitochondrial cytochrome *c*, because PAM detects endogenous optical absorption with a relative sensitivity of 100%[11]. In biological tissue, hemoglobin and melanin are two major sources of endogenous optical absorption in the visible spectral range. So PAM has found broad applications in structural and functional vascular imaging and melanoma tumor imaging *in vivo*[12][13]. Recently, more contrasts have been explored for photoacoustic tomography, such as DNA and RNA in nuclei[14] by using ultraviolet (UV) illumination and water[15] and lipid[16] by using near-infrared illumination. Here, we showed for the first time that PAM can also be applied to label-free imaging of cytochrome *c* in cells by using its optical absorption around the Soret peak (~415 nm).

2. MATERIALS AND METHODS

Fig. 1 shows the PAM system for cytochrome *c* imaging. We used an integrated diode-pumped laser and optical parametric oscillator system (NT242-SH, Ekspla), which had a tunable wavelength range from 210 nm to 2600 nm. The laser pulses had a pulse width of 5 ns and a repetition rate of 1 KHz. The laser pulses were focused by a condenser lens

Photons Plus Ultrasound: Imaging and Sensing 2012, edited by Alexander A. Oraevsky, Lihong V. Wang,
Proc. of SPIE Vol. 8223, 82231W · © 2012 SPIE · CCC code: 1605-7422/12/$18 · doi: 10.1117/12.906202

and filtered by a 50 μm pinhole, which worked as a point source for the optical objective. Compared with a fiber-based light delivery system[17], this free-space system provides both greater tolerance of beam shifting and easier optical alignment, especially for a large range of wavelength tuning. We used a 0.60 numerical aperture (NA) objective for visible light (46 07 15, Zeiss) and a 0.40 NA objective (LMU-20X-UVB, Thorlabs) for UV light. The pulses focused by the objective irradiated on the sample and generated photoacoustic waves, whose amplitude was proportional to the localized optical absorption at the focal point. A focused ultrasonic transducer (customized with 40 MHz central frequency, 80% bandwidth, and 0.50 NA) detected the photoacoustic waves in the transmission mode. The signals from the transducer were then amplified and digitized at 1 GS/s (PCI-5152, National Instruments). The sample was mechanically scanned, and the 2D maximum-amplitude projection (MAP) images of the sample could be obtained.

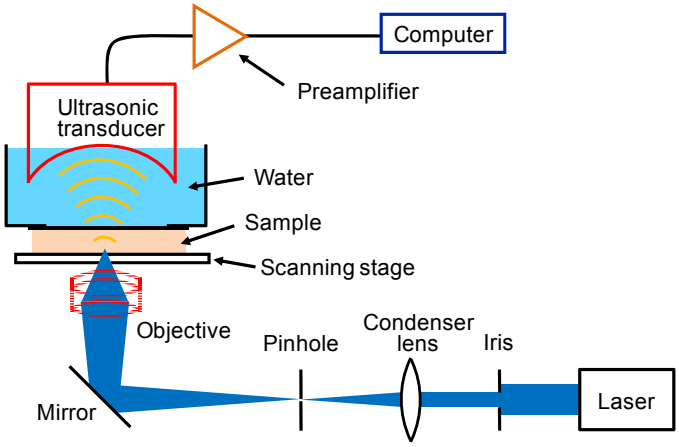

Figure 1. System schematic of photoacoustic microscopy.

For cytochrome *c* imaging, the wavelength of the laser was set to 422 nm, slightly away from the absorption peak of cytochrome *c*. This is because the laser provides higher pulse energy and better power stability at 422 nm than the exact Soret peak. The wavelength was set to 250 nm for cell nuclei imaging due to the strong DNA and RNA absorption.

3. RESULTS AND DISCUSSION

Unstained fibroblasts (NIH/3T3, ATCC) were imaged by PAM. The fibroblasts were seeded onto the quartz cover glasses at a density of 2×10^4 cells/cm^2 and fixed in 3.7% formaldehyde for the imaging experiments. The mitochondrial cytochrome *c* in fibroblasts were imaged by PAM with 422 nm wavelength and 200 nJ pulse energy, as shown in green in Fig. 2(a). Inside each cell there was a dark hole, which should be the nucleus. As a validation, the fibroblasts were imaged again with 250 nm wavelength, as shown in Fig. 2(b), where the nuclei were shown in blue. Fig. 2(c) was a superimposed image of Figs. 2(a) and (b). As a comparison, the cells were then stained with MitoTracker Green FM® (Invitrogen) for mitochondria and 4',6-diamidino-2-phenylindole (Invitrogen) for nuclei. Fig. 2(d) shows the fluorescence image of the stained cells, which matches well with the PAM image shown in Fig. 2(c). Therefore, PAM can be used for label-free imaging of cytochrome *c* in fibroblasts. Here individual mitochondria were not resolved by either PAM or fluorescence microscopy due to the insufficient axial resolution. When imaging the cells, all the mitochondria were projected along the depth direction and were thereby mixed together. However, individual mitochondria were resolved by confocal optical microscopy due to its finer axial resolution, as shown in Fig. 2(e).

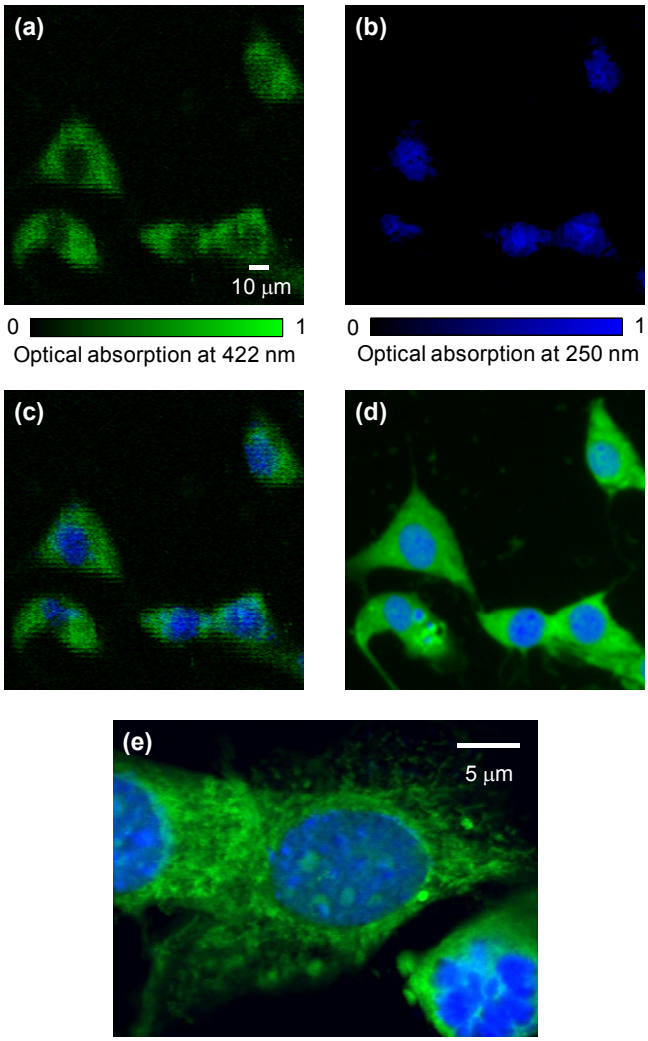

Figure 2. PAM and fluorescence microscopy of fibroblasts. (a) Label-free PAM image of fixed but unstained fibroblasts at 422 nm wavelength. (b) Label-free PAM image at 250 nm wavelength. (c) Superimposed image of (a) and (b). (d) Wide-field fluorescence image of the cells with mitochondria stained in green and nuclei stained in blue. (e) Confocal microscopy image of the stained cells.

A histological section of a mouse ear was imaged by label-free PAM. All experimental animal procedures were carried out in conformity with the laboratory animal protocol approved by the Animal Studies Committee of Washington University in St. Louis. Fig. 3(a) shows the label-free PAM image of a mouse (Hsd:ND4, Harlan Co.) ear section acquired at 422 nm wavelength. Lots of structures were identified from the PAM image. The hemoglobin in blood vessels had the strongest optical absorption. The connective tissue and the auricular cartilage were clearly imaged. The most common cells in connective tissue are fibroblasts, and the auricular cartilage is one kind of connective tissue. Compared with the connective tissue, the muscle cells generated stronger signals, because the muscle cells have a greater demand for ATP and, therefore, contain more mitochondria. Then the mouse ear section was stained with hematoxylin and eosin. The optical microscopy image of the stained section [Fig. 3(b)] matched well with the unstained PAM image. Therefore, PAM has the potential for label-free histology. With proper wavelengths, PAM can image various substance of interest, including cytochrome *c*, DNA, RNA, lipid, hemoglobin, melanin, etc.

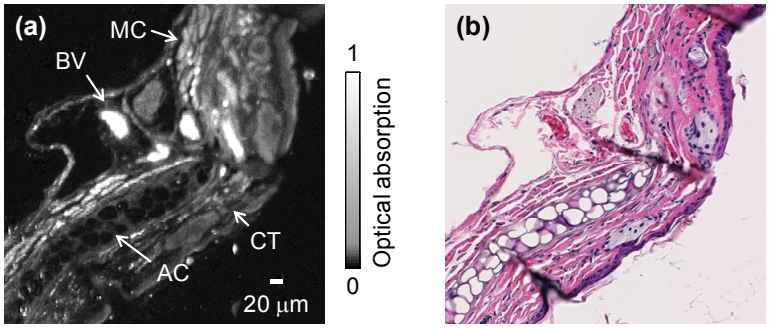

Figure 3. Histological section of mouse ear. (a) Label-free PAM image acquired at 422 nm wavelength. BV: blood vessel. MC: muscle cell. CT: connective tissue. AC: auricular cartilage. (b) Optical microscopy image acquired with hematoxylin and eosin staining.

4. CONCLUSIONS

In summary, we realized label-free PAM of cytochrome *c* in cells for the first time. Label-free PAM can be further developed for real-time imaging of cytochrome *c* functions in live cells or *in vivo*. First, in order to have a better axial resolution, we can use a broadband piezoelectric transducer or microring resonator[18]. Second, in order to enhance the imaging speed, we can combine a high-repetition-rate laser with laser scanning[19] or voice-coil scanning[20].

ACKNOWLEDGMENTS

This work was sponsored in part by National Institutes of Health grants R01 EB000712, R01 EB008085, R01 CA134539, U54 CA136398, R01 CA157277, and 5P60 DK02057933. L.W. has a financial interest in Microphotoacoustics, Inc. and Endra, Inc., which, however, did not support this work.

REFERENCES

[1] Gupte, S. S. and Hackenbrock, C. R., "The role of cytochrome *c* diffusion in mitochondrial electron transport," J. Biol. Chem. 263(11), 5248–5253 (1988).
[2] Liu, X., Kim, C. N., Yang, J., Jemmerson, R. and Wang, X., "Induction of apoptotic program in cell-free extracts: requirement for dATP and cytochrome c," Cell 86(1), 147–157 (1996).
[3] Cipolat, S., Rudka, T., Hartmann, D., Costa, V., Serneels, L., *et al.*, "Mitochondrial rhomiboid PARL regulates cytochrome c release during apoptosis via OPA-1 dependent cristae remodeling," Cell 126(1), 163–175 (2006).
[4] Vaughn, A. E. and Deshmukh, M., "Glucose metabolism inhibits apoptosis in neurons and cancer cells by redox inactivation of cytochrome *c*," Nat. Cell Biol. 10, 1477–1483 (2008).
[5] Scorrano, L., Petronilli, V., Colonna, R., Lisa, F. D. and Bernardi, P., "Chloromethyltetramethylrosamine (Mitotracker Orange™) induces the mitochondrial permeability transition and inhibits respiratory complex I. Implications for the mechanism of cytochrome *c* release," J. Biol. Chem. 274(35), 24657–24663 (1999).
[6] Buckman, J. F., Hernández, H., Kress, G. J., Votyakova, T. V., Pal, S. and Reynolds, I. J., "MitoTracker labeling in primary neuronal and astrocytic cultures: influence of mitochondrial membrane potential and oxidants," J. Neurosci. Method. 104(2), 165–176 (2001).
[7] Tamaki, E., Sato, K., Tokeshi, M., Sato, K., Aihara, M. and Kitamori, T. "Single-cell analysis by a scanning thermal lens microscope with a microchip: direct monitoring of cytochrome *c* distribution during apoptosis process," Anal. Chem. 74(7), 1560–1564 (2002).
[8] Brusnichkin, A. V., Nedosekin, D. A., Galanzha, E. I., Vladimirov, Y. A., Shevtsova, E. F., *et al.*, "Ultrasensitive label-free photothermal imaging, spectral identification, and quantification of cytochrome *c* in mitochondria, live cells, and solutions," J. Biophotonics 3(12), 791–806 (2010).

[9] Thorell, B. and Chance, B., "Microspectrography of respiratory enzymes within the single, mammalian cell under different metabolic conditions," Exp. Cell Res. 20(1), 43–55 (1960).
[10] Thorell, B., Chance, B. and Legallais, V., "Microspectrophotometry of cytochromes in the single cell at room and liquid nitrogen temperatures," J. Cell Biol. 26(3), 741–746 (1965).
[11] Wang, L. V., "Multiscale photoacoustic microscopy and computed tomography," Nat. Photon. 3(9), 503–509 (2009).
[12] Zhang, H. F., Maslov, K., Stoica, G. and Wang, L. V., "Functional photoacoustic microscopy for high-resolution and noninvasive *in vivo* imaging," Nat. Biotech. 24, 848–851 (2006).
[13] Zhang, C., Maslov, K. and Wang, L. V., "Subwavelength-resolution label-free photoacoustic microscopy of optical absorption *in vivo*," *Opt. Lett.* **35**(19), 3195–3197 (2010).
[14] Yao, D.-K., Maslov, K., Shung, K. K., Zhou, Q. and Wang, L. V., "*In vivo* label-free photoacoustic microscopy of cell nuclei by excitation of DNA and RNA," Opt. Lett. 35(24), 4139–4141 (2010).
[15] Xu, Z., Zhu, Q. and Wang, L. V., "*In vivo* photoacoustic tomography of mouse cerebral edema induced by cold injury," J. Biomed. Opt. 16(6), 066020–1–5 (2011).
[16] Wang, H.-W., Chai, N., Wang, P., Hu, S., Dou, W., *et al.*, "Label-free bond-selective imaging by listening to vibrationally excited molecules," Phy. Rev. Lett. 106(23), 238106–1–4 (2011).
[17] Hu, S., Maslov, K. and Wang, L. V., "Second-generation optical-resolution photoacoustic microscopy with improved sensitivity and speed," Opt. Lett. 36(7), 1134–1136 (2011).
[18] Xie, Z., Chen, S.-L., Ling, T., Guo, L. J., Carson, P. L. and Wang, X., "Pure optical photoacoustic microscopy," Opt. Express 19(10), 9027–9034 (2011).
[19] Rao, B., Maslov, K., Danielli, A., Chen, R., Shung, K. K., *et al.*, "Real-time four-dimensional optical-resolution photoacoustic microscopy with Au nanoparticle-assisted subdiffraction-limit resolution," Opt. Lett. 36(7), 1137–1139 (2011).
[20] Wang, L., Maslov, K., Yao, J., Rao, B. and Wang, L. V., "Fast voice-coil scanning optical-resolution photoacoustic microscopy," Opt. Lett. 36(2), 139–141 (2011).